

# A Terminal Guidance Technique for Lunar Landing

S J CITRON,\* S E DUNIN,† and H F MEISSINGER‡

*Hughes Aircraft Company, El Segundo, Calif*

Terminal guidance of a soft-landing lunar spacecraft can be achieved by perturbing a nominal gravity-turn trajectory. This perturbation is imposed by offsetting the thrust vector for some period of time from the nominal attitude, anti-parallel to the instantaneous velocity vector. The offset is removed when the predicted and required landing points coincide. The vehicle then proceeds along a gravity-turn descent trajectory until landing. Closed-form solutions obtained determine the thrust acceleration required and the predicted landing-point coordinates. For trajectories following a shallow descent, as from a parking orbit, the moon is represented by spherical geometry. For trajectories that initially make large angles with the local horizon, or have small velocities, the moon is considered flat. During descent an on-board computer compares the predicted and desired landing-point coordinates. A pin-point guidance channel drives the down-range and cross-range components of the landing point error to zero. A soft-landing control channel constrains the thrust level so as to terminate the trajectory at the lunar surface with zero velocity. Separation of the two control functions has the advantage of assuring a safe landing in the event of component failures in the pin-point guidance subsystem. Simulation studies have shown this technique to be quite effective.

## Nomenclature

$a$	= thrust acceleration
$E$	= vehicle energy per unit mass
$g_n$	= acceleration at lunar surface due to gravitational attraction, 5 322 ft/sec <sup>2</sup>
$H = r^2\dot{\theta}$	= vehicle angular momentum
$h$	= altitude above lunar surface
$r$	= radial distance from center of moon
$r_n$	= lunar radius 5 702 $\times 10^6$ ft
$s$	= path length traversed
$t$	= time
$V$	= vehicle velocity
$V_c = [\mu/r]^{1/2}$	= circular velocity
$V_{ff} = [2g_n h_0]^{1/2}$	= free-fall velocity
$x$	= down-range distance traversed at any time during descent, flat moon
$y$	= height above lunar surface, flat moon
$\gamma$	= flight path angle
$\theta$	= central angle traversed by vehicle at any time during descent
$\mu$	= lunar gravitational parameter
$\rho = g_n/a$	= reciprocal of normalized thrust acceleration

## Subscripts

0	= initial value
f	= value at termination of landing maneuver

## Problem Statement

PREVIOUS analyses of the lunar problem have been principally concerned with either the basic trajectory considerations for various types of approach<sup>1-3</sup> or implicit guid-

Presented as Preprint 2685-62 at the ARS 17th Annual Meeting and Space Flight Exposition, Los Angeles, Calif., November 13-18, 1962; revision received December 16, 1963. The authors wish to acknowledge the support of the technical staff of Hughes Aircraft Company. The cooperation of Lynn Grasshoff, who was responsible for formulating and directing simulation studies of a manually controlled pin point landing system embodying the techniques mentioned in this paper, has been particularly appreciated.

\* Senior Staff Consultant, Aerospace Group, Space Systems Division; also Associate Professor, Purdue University, Lafayette, Ind.

† Head, Astrodynamics Section, Aerospace Group, Space Systems Division.

‡ Manager, Space Guidance Staff, Aerospace Group, Space Systems Division; now with Space Technology Laboratories, Inc., Redondo Beach, Calif.

ance systems with varying amounts of landing-point prediction capability.<sup>4-8</sup> The attendant complexity of some of these systems, which require high-speed repetitive computation, has led the authors to consider the possibility of developing an explicit guidance technique.

It is the purpose of this paper to present a method of accomplishing soft landings at predetermined points on the lunar surface. The guidance system used is self-contained and may be applied to either a hyperbolic approach or a descent from a parking orbit.

In addition to the analytical determination of the descent trajectories, a possible system implementation of the pin-point landing scheme is described. Requirements for on-board sensing and navigation equipment are established, and procedures for automatic and manual guidance operations are discussed. Results showing the effectiveness of the guidance scheme for a variety of initial conditions and with various forms of thrust control are presented.

## Method of Solution

The means used to assure soft landing consists of the continuous application of retrothrust in a direction opposite to the velocity vector during the descent phase. For a suitably chosen thrust level the resultant gravity turn terminates in a vertical landing at zero speed. The foregoing technique does not, however, assure a landing at or near the chosen location owing to accumulated uncorrected navigation and guidance errors.

To augment the soft-landing scheme to include the capacity of "pin-point" guidance, the following technique is used. The thrust vector is offset from its nominal orientation anti-parallel to the velocity vector, thus providing a controlled pitch or yaw maneuver. This modified gravity turn continues until predicted down-range and cross-range landing-point errors are reduced to zero. The thrust offset is then removed and the remainder of the descent again follows a nominal gravity turn. Simulation studies have shown this technique to be quite effective.

The technique has been developed for use in manned and unmanned lunar-landing vehicles. It lends itself to guidance and control of the descent either directly from a hyperbolic approach, or from a parking orbit, which is the preferred approach for manned missions. A relatively simple on-board computer using the analytic solutions developed continuously predicts the location of the soft-landing point.

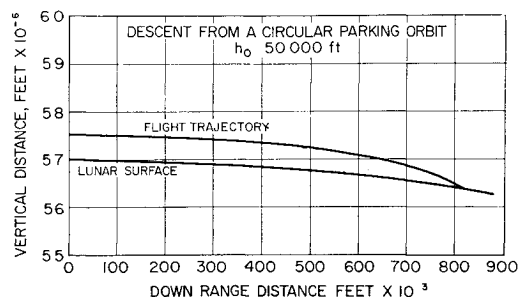


Fig 1 Gravity-turn descent from a circular parking orbit ( $h_0 = 50,000$  ft)

These landing coordinates, i.e., those that would occur if the gravity turn were continued, are then compared with the desired landing-site coordinates. The predicted error in the landing site determines the necessary thrust offset from the velocity vector in pitch and yaw. During this operation two feedback loops are operative: soft-landing control and pin-point guidance. The function of the soft-landing control is to maintain the thrust level at a value that assures termination of descent at zero velocity and zero altitude.<sup>§</sup> The function of the pin-point guidance system is to drive the down-range and cross-range components of the landing-point error to zero. Separation of the two control functions has the advantage of assuring a safe landing in the event of component failure in the pin-point landing subsystem.

Analytical solutions are obtained to determine the thrust acceleration level required for soft landing at any time during descent and to provide the predicted landing point so that any deviation from the desired landing point may be corrected. The problem is considered in two parts. For trajectories that initially make small angles with the local horizontal (shallow descent as from a parking orbit) and that have velocities greater than the free-fall velocity, the gravity-turn problem is approximately solved using the circular geometry of the moon. For trajectories that initially make large angles with the local horizontal or those that make small angles but have velocities no larger than the free-fall velocity, the gravity-turn problem is exactly solved using a flat moon geometry. The guidance scheme based on closed-form expressions obtained from both models is shown to be convergent, improving in accuracy as the altitude approaches zero. By comparison of the results with digital computer solutions of the exact equations of motion, confirmation of the models used was provided.

### Trajectory Analysis

The trajectory analysis provides the vehicle on-board computer with closed-form expressions for the predicted landing point and the correct constant thrust-acceleration level for gravity-turn descent. Corresponding to either shallow or steep descents, the mathematical models considered use a circular or flat geometry for the moon, respectively. Since in the terminal phase of all descents the surface approaches the flat geometry, the two solutions are complementary and cover the range of possible trajectories. Further aspects of the gravity-turn descent are considered in the Appendix.

### Spherical Moon

The equations of motion in cylindrical coordinates with the thrust acceleration anti-parallel to the velocity vector are

<sup>§</sup> In practice, the vehicle would be made to hover at some height greater than zero. As no additional difficulty is encountered by requiring that the velocity be zero for some  $h > 0$ , it is sufficient for the purpose of this paper to let the descent end (zero velocity) at zero altitude.

$$\ddot{r} - (H^2/r^3) = -(\mu/r^2) - (a\dot{r}/V) \quad (1a)$$

$$\dot{H} = -a(H/V) \quad (1b)$$

The instantaneous rate of increase of the vehicle's energy per unit mass is

$$\dot{E} = -aV \quad (2)$$

Changing the independent variable from time to path length we obtain

$$dE/ds = -a \quad (3)$$

which may be directly integrated, yielding

$$E = -as + E_0 = -as + V_0^2/2 - \mu/r_0 \quad (4)$$

The expression for the square of the velocity as a function of path length is thus

$$V^2 = -2as + V_0^2 + 2\mu[(r_0 - r)/rr_0] \quad (5)$$

Since  $h/r \ll 1$ , the expression for  $V^2$  to order  $(h/r)$  becomes

$$V^2 = -2as + V_0^2 + 2g_m(h_0 - h) \quad (6)$$

The terminal condition is that  $V = 0$  and  $h = 0$ , when  $s = s_f$ , the total path length. Therefore, with no further approximation,

$$s_f = (V_0^2 + 2g_m h_0)/2a \quad (7)$$

For use with circular moon geometry, only those trajectories are considered whose initial velocity is greater than the free-fall velocity.<sup>¶</sup> Under this assumption the representation of  $h(s)$  in Eq 6 is not critical, and the simplest  $h(s)$  satisfying initial and final conditions is assumed

$$h = h_0[1 - (s/s_f)] \quad (8)$$

Therefore, substitution of Eqs (7) and (8) into Eq (6) yields

$$V^2 = V_0^2[1 - (s/s_f)] \quad (9)$$

Changing the independent variable from  $t$  to  $s$  in Eqs (1a) and (1b) yields

$$rV^2(d^2r/ds^2) = [1 - (dr/ds)^2][V^2 - (\mu/r)] \quad (10a)$$

$$dH/ds = -aH/V^2 \quad (10b)$$

The problem thus requires the solution of Eq (10a) for the determination of the value of thrust acceleration  $a$  terminating the trajectory with zero velocity at the lunar surface ( $r = r_m$ ). The solution of Eq (10b) then yields the down-range distance traversed on the circular moon and provides the landing-point prediction equation.

Since, as may be shown analytically,  $dr/ds$  is nearly equal to its initial value over most of the path for trajectories whose initial velocities are greater than the free-fall velocity,  $dr/ds$

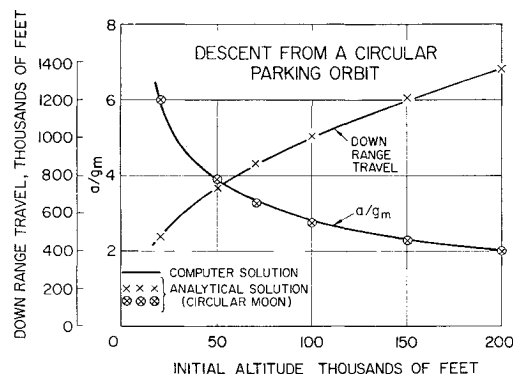


Fig 2 Analytical and computer solutions for thrust acceleration and down-range travel for gravity-turn descents from a circular parking orbit (circular moon model)

<sup>¶</sup> For a circular orbit at 50,000 ft,  $V_0^2/V_{ff}^2 = 56$

is replaced by  $(dr/ds)_0$  in Eq (10a) (see Fig 1) Further, as the change in  $r$  is only of the order of 3% for initial altitudes up to 200,000 ft,  $r$  is replaced by  $r_m$  in Eq (10a)

Defining the flight path angle  $\gamma$  by

$$\sin \gamma = \dot{r}/V = dr/ds \quad (11)$$

Eq (10a) becomes

$$\frac{r_m}{\cos^2 \gamma_0} \frac{d^2 \gamma}{ds^2} = 1 - \frac{\mu/r_m}{V_0^2 [1 - (s/s_f)]} \quad (12)$$

Integrating twice, subject to the conditions  $r = r_0$ ,  $dr/ds = \sin \gamma_0$  when  $s = 0$ , yields

$$\frac{1}{\cos^2 \gamma_0} [r - s \sin \gamma_0] = \frac{s^2}{2r_m} - \frac{g_m s_f}{V_0^2} s - \frac{g_m s_f^2}{V_0^2} \left(1 - \frac{s}{s_f}\right) \ln \left(1 - \frac{s}{s_f}\right) + \frac{r_0}{\cos^2 \gamma_0} \quad (13)$$

Setting  $r = r_0 - h_0$ ,  $s = s_f$  in Eq (13), and substituting for  $s_f$  from Eq (7), a quadratic equation is obtained which yields the thrust acceleration  $a$  required to terminate the descent on the moon's surface with zero velocity The equation is

$$\frac{a^2}{g_m^2} + \sin \gamma_0 \left[ \frac{V_0^2}{2h_0 g_m} + 1 \right] \frac{a}{g_m} - \frac{\cos^2 \gamma_0}{4V_0^2 h_0 g_m} [V_0^2 + 2g_m h_0]^2 \left[ 1 - \frac{V_0^2}{2r_m g_m} \right] = 0 \quad (14)$$

For initial velocities less than escape velocity only one positive root exists, and no ambiguity in selection of the correct thrust acceleration occurs A comparison of the results of Eq (14) for descent starting from circular velocity in a parking orbit with a computer solution to the exact equations is given in Fig 2 Excellent agreement is obtained

The landing-point prediction equation remains to be found Substitution of Eq (9) into Eq (10b) and integration subject to the conditions that  $H = H_0$  when  $s = 0$  yields

$$H = r^2 \dot{\theta} = H_0 [1 - (s/s_f)]^{K_1} \quad K_1 = as_f/V_0^2 \quad (15)$$

Changing  $\dot{\theta}$  to  $(d\theta/ds)V$ , substituting for  $V$  from Eq (9), and integrating, holding  $r$  at its initial value  $r_0$ , we find

$$r_0^2 \theta = - \frac{s_f H_0 V_0}{V_0^2 + g_m h_0} \left\{ \left[ 1 - \frac{s}{s_f} \right]^{K_2} - 1 \right\} \quad (16)$$

$$K_2 = \frac{g_m h_0}{V_0^2} + 1$$

where  $\theta = 0$  when  $s = 0$

Setting  $H_0 = r_0 V_0 \cos \gamma_0$ ,  $s = s_f$ , and substituting from Eq (7) for  $s_f$ , the down-range travel along the surface to the landing point is given by

$$r_m \theta_f = \frac{V_0^2}{2a} \cos \gamma_0 \left\{ \frac{V_0^2 + 2g_m h_0}{V_0^2 + g_m h_0} \right\} \left[ \frac{r_m}{r_0} \right] \quad (17)$$

A comparison of this approximate solution for down-range travel with computer solutions of the exact equations starting from circular velocity in a parking orbit is shown in Fig 2 The agreement is again excellent

Although the time of descent is not a necessary input to the guidance scheme, it is an interesting quantity to obtain Integrating Eq 9, realizing that  $V = ds/dt$  and that when  $s = 0$ ,  $t = 0$ , we find

$$s = V_0 t - (V_0^2 t^2 / 4s_f) \quad (18)$$

Setting  $s = s_f$ , the time of descent becomes

$$t_f = 2s_f / V_0 \quad (19)$$

At 50,000 ft for descent from a circular parking orbit, the

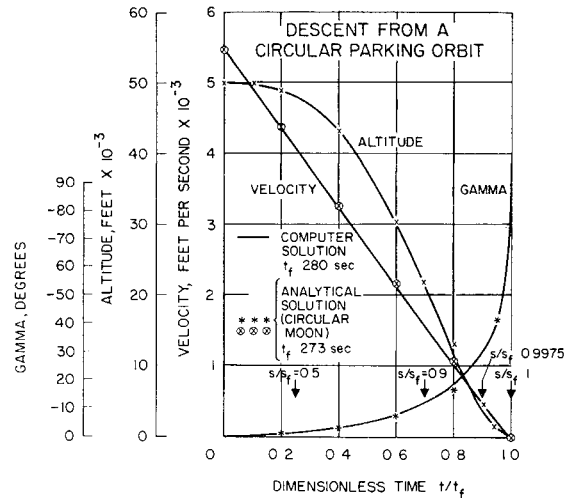


Fig 3 Analytical and computer solutions for velocity, altitude, and flight path angle profiles for gravity-turn descents from a 50,000-ft circular parking orbit (circular moon model)

error in descent time is 2% If greater accuracy is desired, a better approximation may be found by improving the representation of  $h(s)$  in Eq (6)

The characteristic velocity required for the descent is determined by multiplying the thrust acceleration  $a$  by the time of flight  $t_f$  Substituting from Eq (7) for  $s_f$  in Eq (19), the characteristic velocity is given by

$$at_f = V_0 + (2g_m h_0 / V_0) \quad (20)$$

The result is exact if the descent is vertical and may be expected to have the same order of error as  $t_f$  in other cases

As a further check on the validity of the solutions obtained, a comparison was made between computer and analytical solutions of the trajectory characteristics during descent from a circular parking orbit For an initial altitude of 50,000 ft curves of altitude, velocity and flight path angle vs time obtained from both the computer and analytical solutions are shown in Fig 3

The validity of the solution for the thrust acceleration  $a$  as a function of initial velocity for given initial altitude and flight path angle is shown by Fig 4 It is of interest to note that, for a zero initial flight path angle, the required thrust acceleration increases with increasing velocity to a maximum at the circular velocity and then decreases for higher (supercircular) velocities until a direct gravity-turn descent is no longer possible The decrease in the required thrust acceleration may be explained by noting that, for supercircular initial velocities, the vehicle altitude at first increases resulting in a greatly extended path length over which the thrust acceleration may act to reduce the velocity

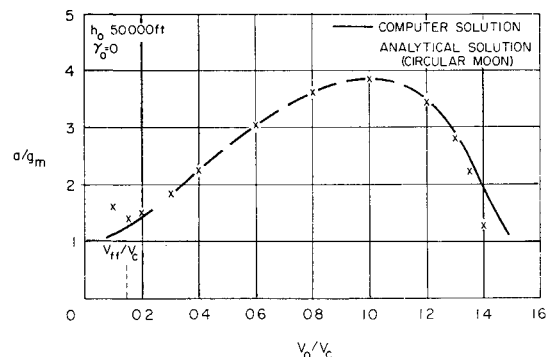


Fig 4 Analytical and computer solutions for thrust acceleration as a function of initial velocity (circular moon model)

### Flat Moon

A rectangular coordinate system is used with origin on the surface of the moon, the  $y$  axis along the local vertical, and the  $x$  axis in the plane defined by the local vertical and the velocity vector. The equations of motion with the thrust acceleration anti-parallel to the velocity vector are

$$\ddot{y} = -(ay/V) - g_m \quad (21a)$$

$$\ddot{x} = -a\dot{x}/V \quad (21b)$$

Consistent with the restriction of a flat lunar geometry a constant gravity field is used. Dividing Eq (21a) by Eq (21b) yields

$$dy/d\dot{x} = (y/\dot{x}) + (g_m/a)[1 + (y/\dot{x})^2]^{1/2} \quad (22)$$

Solving Eq (22) we find

$$y = \dot{x} \sinh[\ln C \dot{x}^\rho] = \frac{C}{2} \dot{x}^{(1+\rho)} - \frac{1}{2C} \dot{x}^{(1-\rho)} \quad (23)$$

where

$$\rho = g_m/a \quad (24)$$

$$C = \dot{x}_0^{-\rho} \lambda$$

$$\lambda = (y_0 + V_0)/\dot{x}_0$$

Equation (23) suffices to yield the velocity profile during descent. In particular we note that

$$V = [\dot{x}^2 + y^2]^{1/2} \quad (25)$$

$$= \dot{x} \cosh[\ln C \dot{x}^\rho]$$

Combining Eqs (21b) and (25) we obtain

$$d\dot{x}/dt[1 + (y/\dot{x})^2]^{1/2} = -a \quad (26)$$

$$\cosh[\ln C \dot{x}^\rho] d\dot{x} = -adt$$

$$\frac{1}{2} \left[ \lambda \left( \frac{\dot{x}}{\dot{x}_0} \right)^\rho + \frac{1}{\lambda} \left( \frac{\dot{x}}{\dot{x}_0} \right)^{-\rho} \right] d\dot{x} = -adt$$

Integrating, subject to the condition  $\dot{x} = \dot{x}_0$  when  $t = 0$ ,

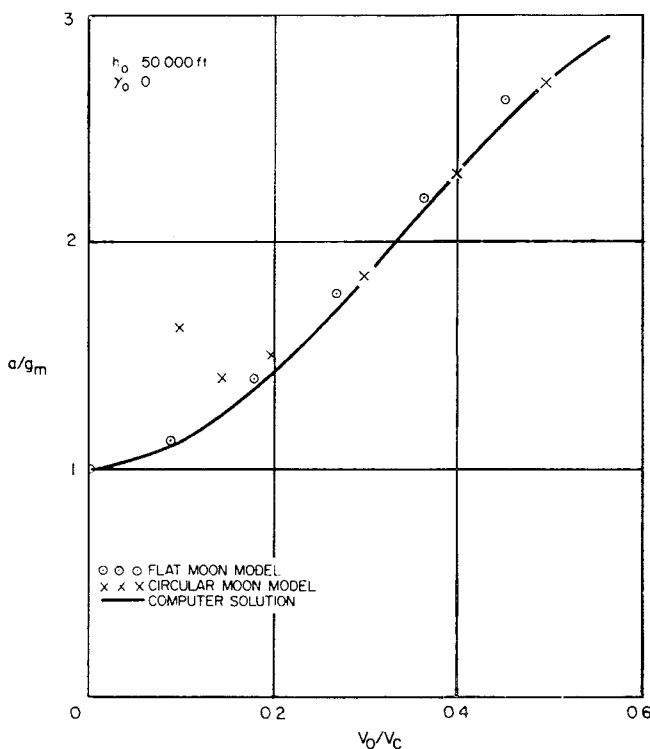


Fig 5 Analytical and computer solutions for thrust acceleration as a function of initial velocity. Comparison of flat and circular moon models

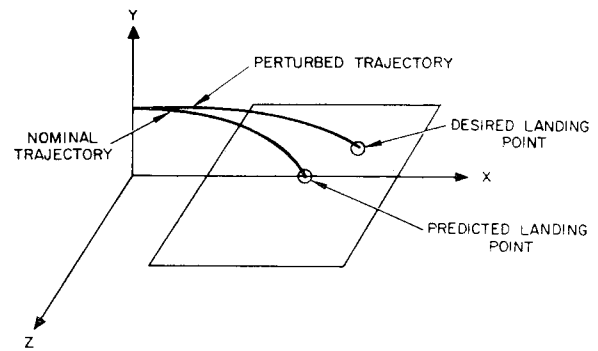


Fig 6 Landing maneuver

yields

$$\frac{\dot{x}}{2} \left[ \frac{\lambda (\dot{x}/\dot{x}_0)^\rho}{(1+\rho)} + \frac{(\dot{x}/\dot{x}_0)^{-\rho}}{\lambda(1-\rho)} \right] - \frac{\dot{x}_0}{2} \left[ \frac{\lambda}{(1+\rho)} + \frac{1}{\lambda(1-\rho)} \right] = -at \quad (27)$$

Noting that

$$d\dot{x}/dx = -a/V \quad (28)$$

$$d\dot{x}/dy = -(a/V)(\dot{x}/y)$$

differential equations relating  $y$  and  $x$  to  $\dot{x}$  are obtained. Thus,

$$\dot{x}[1 + (y/\dot{x})^2]^{1/2} d\dot{x} = -adx \quad (29a)$$

$$y[1 + (y/\dot{x})^2]^{1/2} d\dot{x} = -ady \quad (29b)$$

Using the results of Eqs (23) and (25), integration of Eq (29) subject to the condition  $x = 0, y = h_0$  when  $\dot{x} = \dot{x}_0$  yields

$$-ax = \frac{\dot{x}^2}{2} \left[ \frac{\lambda (\dot{x}/\dot{x}_0)^\rho}{(2+\rho)} + \frac{(\dot{x}/\dot{x}_0)^{-\rho}}{\lambda(2-\rho)} \right] - \frac{\dot{x}_0^2}{2} \left[ \frac{\lambda}{(2+\rho)} + \frac{1}{\lambda(2-\rho)} \right] \quad (30a)$$

$$-a[y - h_0] = \frac{\dot{x}^2}{8} \left[ \frac{\lambda^2 (\dot{x}/\dot{x}_0)^{2\rho}}{(1+\rho)} - \frac{(\dot{x}/\dot{x}_0)^{-2\rho}}{\lambda^2(1-\rho)} \right] - \frac{\dot{x}_0^2}{8} \left[ \frac{\lambda^2}{(1+\rho)} - \frac{1}{\lambda^2(1-\rho)} \right] \quad (30b)$$

Eqs (27, 30a, and 30b) completely specify the trajectory.

The thrust-acceleration level for termination at the lunar surface with zero velocity is obtained from Eq (30b) by putting  $y = 0, x = 0$ . The equation resulting is

$$\frac{a^2}{g_m^2} + \sin^2 \gamma_0 \left[ \frac{V_0^2}{2h_0 g_m} \right] \frac{a}{g_m} - \left[ \frac{V_0^2(1 + \sin^2 \gamma_0)}{4h_0 g_m} + 1 \right] = 0 \quad (31)$$

Only one positive root exists. Thus, no ambiguity in selection of the correct thrust acceleration occurs.

The thrust acceleration required as a function of initial velocity is compared in Fig 5 with that required by the exact computer solution and the solution using the circular lunar geometry. The overlapping of the regions of applicability of the flat and circular geometry models indicates the feasibility of a transition between them.

The landing point prediction equation is found by putting  $\dot{x} = 0$  in Eq (30a) yielding

$$x_f = \frac{V_0^2 \cos \gamma_0}{2} \left[ \frac{(1 + \sin \gamma_0)}{2a + g_m} + \frac{(1 - \sin \gamma_0)}{2a - g_m} \right] \quad (32)$$

for the down-range travel from thrust-initiation time until landing

The time for descent is obtained from Eq (27) with  $\dot{x} = 0$

$$t_f = \frac{V_0}{2} \left[ \frac{(1 + \sin \gamma_0)}{a + g_m} + \frac{(1 - \sin \gamma_0)}{a - g_m} \right] \quad (33)$$

The characteristic velocity required for the descent is then given by  $at_f$

A double integration of Eq (21) has appeared previously in the literature<sup>10</sup> The advantage of the parameterization of this paper is that it yields more readily the thrust control Eq (31)

### Guidance Implementation

The terminal descent maneuver, which takes the vehicle to the designated landing site, consists in applying a lateral component of the retrothrust in the direction of the desired shift of the predicted touchdown point, thus perturbing the nominal soft-landing trajectory as illustrated in Fig 6

For retro-engines with fixed thrust orientation, a pitch or yaw attitude change of the vehicle from the nominal tangential thrust orientation accomplishes the desired thrust offset. By restricting the thrust offset to angles of  $10^\circ$  to  $20^\circ$ , a substantial maneuvering capability is gained without major fuel expenditures, since the tangential thrust component remains essentially unchanged while the lateral maneuver is performed. Thus, down-range and cross-range shifts of the touchdown location of 5 to 10 naut miles can be achieved by increasing the total retro-impulse by an amount of only a few hundred feet per second depending upon the initial descent characteristics and the time of initiation of the landing-point correction maneuver (see Fig 7)

Figure 8 shows the configuration of the terminal guidance system used in this study. As shown in the diagram, the touchdown position is predicted by a relatively simple on-board computer based on 1) velocity measurements by a Doppler radar, 2) altitude obtained by means of a radar altimeter, and 3) vehicle attitude, and, hence, flight path angle relative to the local horizon. The latter is obtained from a horizon seeker. With these data, the range prediction equations (17) and (32), derived in the preceding section, yield the down-range distance to touchdown, provided the vehicle continues its descent in a nominal gravity turn at the current setting of retrothrust acceleration.

The desired landing-point position relative to the instantaneous vehicle position is obtained on the basis of updated trajectory information, and the miss distance is determined. Down-range and cross-range components of miss are nulled simultaneously or sequentially by the pitch and yaw guidance channels, respectively.

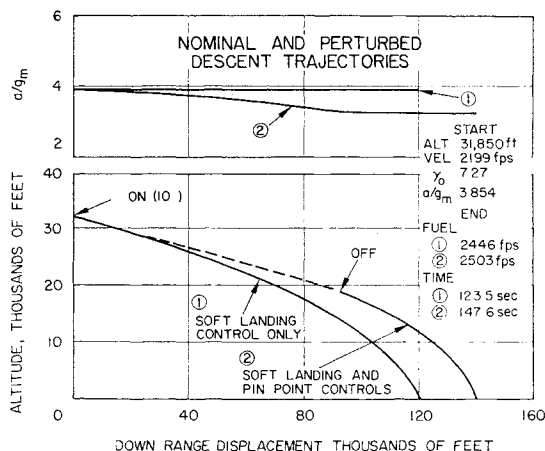


Fig 7 Typical lateral displacement (pin-point landing control)

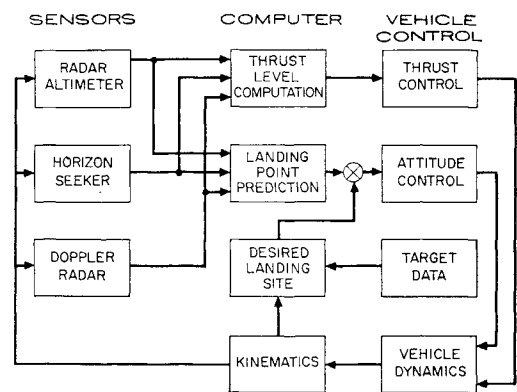


Fig 8 Block diagram of terminal guidance system for pin-point landing

The thrust-acceleration level is adjusted automatically by the closed loop soft-landing control channel. The thrust equations (14) and (31) are used to determine the necessary value of constant retro-acceleration. This assures that the termination point ( $V = 0$ ) is always held at zero altitude.

For any period of true gravity turn the predicted landing point remains fixed, and the thrust acceleration level to achieve soft landing is held constant. During a period of thrust offset the predicted landing point is moving monotonically, and the required thrust level to achieve soft landing varies slowly. The two closed loop systems, soft-landing control and pin-point landing guidance, therefore, interact to some degree. Analysis has shown, however, that this interaction is of no serious consequence from the standpoint of system stability and maneuver accuracy.

The thrust offset employed to yield the desired correction of touchdown location can assume various types of profiles, but for simplicity an offset command at constant level for large error distances and proportionally decreasing for errors below a threshold value was investigated in this study (see Fig 2). The net shift of touchdown location is nearly proportional to the area under the thrust offset curve.

The gradual offset reduction toward the end of the maneuver was introduced to minimize the effect of finite attitude rates upon the final touchdown location resulting from this maneuver. Assuming a first-order time lag in vehicle attitude, the dashed thrust offset curve in Fig 9 is obtained.

In a manned landing vehicle the crew can observe lunar fixes as the landing point is approached and feed this information to the guidance computer. A possible scheme for pilot display is illustrated in Fig 10.

The map display (Fig 10a) shows miss components down-range  $x$  and cross-range  $z$ . The pilot maintains thrust offset until the miss components are reduced to zero. The steering dot display (Fig 10b) shows pitch and yaw offsets  $\alpha$  and  $\beta$ , respectively. The pilot can thus maintain nominal or offset gravity turn by simultaneously observing the two display instruments. An application of the concepts developed here to the command guidance of an unmanned lunar-landing vehicle by an earth-based human operator<sup>11</sup> has been studied analytically and by manned simulation. This guidance system, based on television data display to the human operator, yields extremely high terminal accuracies.

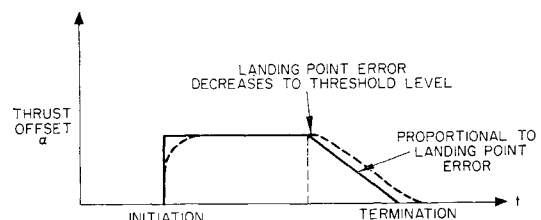


Fig 9 Thrust-offset profile

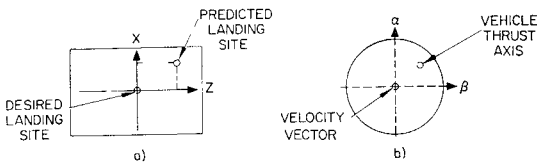


Fig 10 Pilot display instruments

Appendix: Properties of the Offset Gravity-Turn Descent

A study of the velocity hodograph for the gravity-turn maneuvers discussed reveals qualitative and quantitative properties not easily derived by other means. Of some interest are the characteristics of the offset gravity turn for which an explicit solution has not been obtained. The discussion will be restricted to a two-dimensional flat-moon model and is primarily concerned with the terminal landing phase.

The equations governing descent in  $x, y$  coordinates, with a thrust offset from the nominal anti-parallel direction relative to the velocity vector, are given by

$$\begin{aligned} \ddot{y} &= -a \sin(\gamma + \alpha) - g_m \\ \ddot{x} &= -a \cos(\gamma + \alpha) \end{aligned} \tag{A1}$$

where flight path angle  $\gamma$  and thrust offset  $\alpha$  are positive counterclockwise (Fig 11). For convenience of notation the velocity components  $\dot{x}$  and  $\dot{y}$  will be replaced by  $u$  and  $w$ , respectively. The motion will be studied in the  $u, w$  plane (hodograph plane) eliminating time as explicit variable.

The first-order differential equation of hodograph trajectories follows from (A1)

$$\frac{dw}{du} = \frac{\sin(\gamma + \alpha) + \rho}{\cos(\gamma + \alpha)} \tag{A2}$$

where  $\rho = g_m/a$ . The offset angle  $\alpha$  is assumed constant. Substituting  $\sin \gamma = w/V$  and  $\cos \gamma = u/V$  in Eq (A2)

$$\frac{dw}{du} = \frac{w \cos \alpha + u \sin \alpha + \rho V}{u \cos \alpha - w \sin \alpha} \tag{A3}$$

which for small offset angles becomes

$$\frac{dw}{du} = \frac{w + \alpha u + \rho V}{u - \alpha w} \tag{A4}$$

These equations are equivalent to Eq (22) but are stated in a more convenient form for the hodograph analysis.

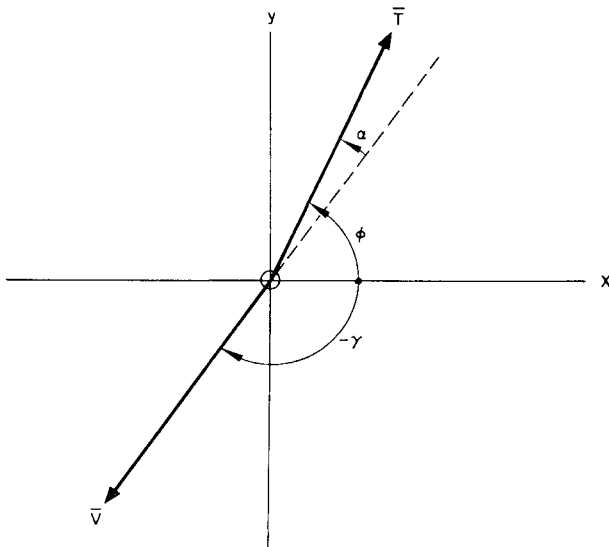


Fig 11 Offset-thrust geometry

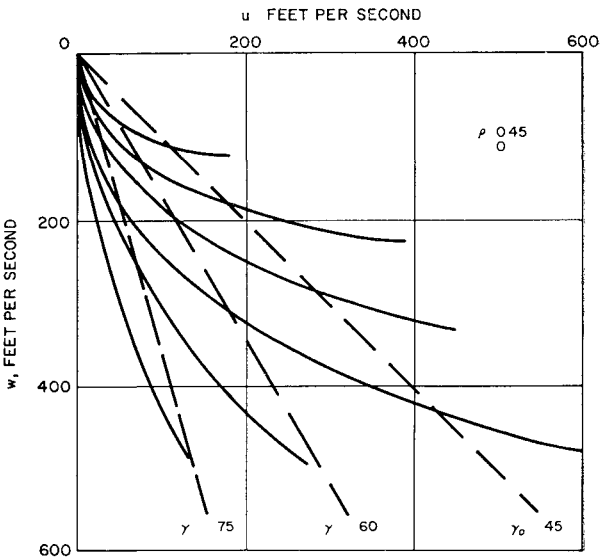


Fig 12 Hodograph trajectories for pure gravity turn

The gravity turn with zero offset is a special case which will be considered first. Equation (A2) reduces to

$$\frac{dw}{du} = \frac{\sin \gamma + \rho}{\cos \gamma} = \frac{w + \rho V}{u} \tag{A5}$$

It is seen that all trajectories must approach the terminal condition  $V = 0$  tangential to the negative  $w$  axis ( $\gamma = -90^\circ$ ), yielding vertical touchdown.

Figure 12 shows a family of trajectories for a given thrust-weight ratio ( $\rho = 0.45$ ). All trajectories go through the origin. Furthermore, they are related to each other through radial scaling, such that all members of the family can be obtained from a particular one by projection along the rays of constant  $\gamma$ . It can be shown that any radius is intersected by every trajectory under the same angle, a property which implies the projective character of the family. This property is useful in allowing construction of many trajectories with only a minimum effort of integration.

Figure 13 shows equivalent trajectories plotted in terms of altitude vs velocity, with flight path angle  $\gamma$  as parameter. (The explicit solutions given by Eqs (25) and (30) were used for this purpose.) The curves of constant  $\gamma$  actually indicate for any velocity and thrust-weight ratio ( $a/g_m$ ), at which altitude the gravity turn must be initiated to lead to zero velocity touchdown. It is interesting to note that the projective character of the hodograph curves in Fig 12 is preserved in the trajectories mapped in Fig 13. The projection is made along the constant  $\gamma$  curves. All descent

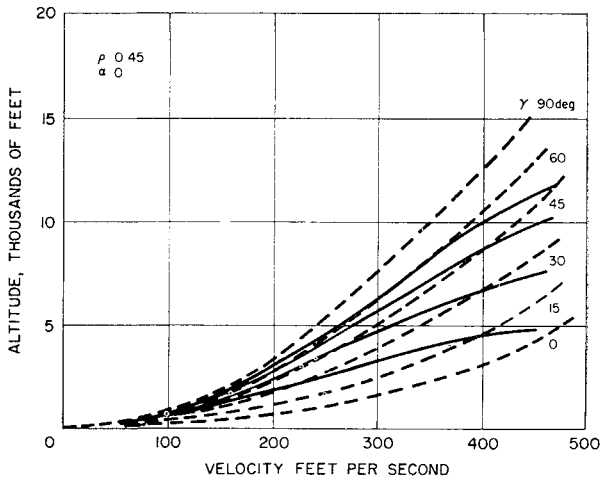


Fig 13 I-h trajectories for pure gravity turn

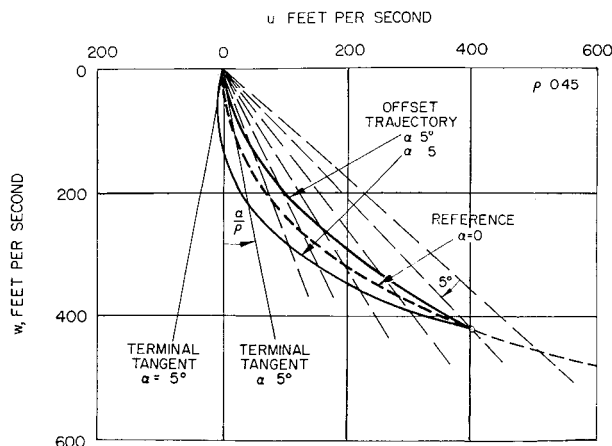


Fig 14 Hodograph trajectories for offset gravity turn ( $\alpha = \pm 5^\circ$ )

curves must approach the line  $\gamma = -90^\circ$  tangentially, as in Fig 12

The foregoing considerations are largely applicable to the offset gravity turn ( $\alpha \neq 0$ ). All trajectories again pass through the origin in the  $u, w$  plane and are related to each other by radial scaling along the lines  $\gamma = \text{const}$ . The terminal angle, however, is no longer  $\gamma = -90^\circ$  but depends on the thrust offset  $\alpha$ . Letting  $V = 0$ , the terminal angle  $\gamma_T$  is obtained from Eq (A4), assuming small values of  $\alpha$ . In the limit, one obtains

$$\lim_{V \rightarrow 0} (dw/du) = \tan \gamma_T \quad (\text{A6})$$

where  $\tan \gamma_T$  satisfies the relation

$$\tan \gamma_T = \frac{\tan \gamma_T + \alpha + \rho / \cos \gamma_T}{1 - \alpha \tan \gamma_T}$$

This yields

$$\cos \gamma_T = -\frac{\alpha}{\rho} \quad (\text{A7})$$

i.e., the terminal angle differs from  $-90^\circ$  as illustrated in Fig 14. Note that theoretically the offset gravity turn may be continued all the way to a terminal condition of soft landing with zero horizontal velocity. For a given thrust offset  $\alpha$ , this would yield a maximum down-range excursion of the landing point. However, according to Eq (A7) the terminal attitude  $\phi_T$  of the vehicle (cf Fig 11) would be

$$\phi_T = \alpha + \cos^{-1} \alpha / \rho \quad (\text{A8})$$

Thus, for typical values of  $\alpha (5^\circ, 15^\circ)$  and  $\rho (0.2, 0.5)$ ,

the vehicle would arrive at a tilt angle too large for safe vertical landing. This condition can be corrected by providing a hover period prior to landing.

It is of some interest that the slope  $dw/du$  of offset gravity-turn trajectories is related to those of pure gravity turn by a rotation through  $\alpha$  according to Eqs (A2) and (A3). It is therefore possible to sketch offset trajectories in the hodograph plane on the basis of reference solutions obtained for  $\alpha = 0$ . The initial and terminal slopes of the offset trajectories as well as slopes at intermediate points are known for given values of  $\alpha$ . Figure 14 shows a reference trajectory (dashed curve) and neighboring offset trajectories (solid curve) indicating the rotation of radii for points of equal slope. Having obtained the deviations of velocity from the reference curve, one can map the offset trajectories in the corresponding  $V-h$  diagram without further numerical work, provided the reference trajectory in that diagram is available.

## References

- 1 Weber, R. J. and Pauson, W. M., "Some thrust and trajectory considerations for lunar landings," NASA TN D-134 (1959).
- 2 Mason, M. and Brainin, S. M., "Descent trajectory optimization for soft lunar landings," *Aerospace Eng.* 21 (April 1962).
- 3 Hakes, R. C., "Guidance and navigation systems for lunar missions," ARS Preprint 2294-61 (1961).
- 4 Queijo, M. J., Miller, Jr., and Kimball, G., "Analysis of two thrusting techniques for soft lunar landings starting from a 50-mile altitude circular orbit," NASA TN D-1230 (1962).
- 5 Green, W. G., "Logarithmic navigation for precise guidance of space vehicles," *Inst. Radio Engrs. Trans. Aerospace Navigational Electron.*, 59-71 (June 1961).
- 6 Kriegsman, B. A. and Reiss, M. H., "Terminal guidance and control techniques for soft lunar landing," *ARS J.* 32, 401-413 (1962).
- 7 Hendrix, C. E., "A soft landing system using optical sensing combining continuously variable thrust," *Proceedings National Winter Conference on Military Electronics* (February 7-9, 1962), pp. 140-145.
- 8 Markson, E. E., Bryant, J. P., and Bergsten, F. C., "Simulation of a manned lunar landing," *AIAA Progress in Astronautics and Aeronautics: Technology of Lunar Exploration*, edited by C. I. Cummings and H. R. Lawrence (Academic Press Inc., New York, 1963), Vol. 10, pp. 561-588.
- 9 Benney, D. J., "Escape from a circular orbit using tangential thrust," *Jet Propulsion* 28, 167-169 (1958).
- 10 Lawden, D. F., "Initial arc of the trajectory of departure," *J. Brit. Interplanet. Soc.* 7, 119-123 (1948).
- 11 Meissinger, H. F., "Lunar landing by command guidance in the presence of transmission time delay," AIAA Preprint 63-346 (1963).